The Comparison in Dehydrogenation Properties and Mechanism between $MgCl_2(NH_3)$/$LiBH_4$ and $MgCl_2(NH_3)$/$NaBH_4$ Systems

L. Gao,[†] Y. H. Guo,[†] Q. Li,[‡] and X. B. Yu*,[†]

Department of Materials Science, Fudan University, Shanghai, China, 200433, and Shanghai Key Laboratory of Modern Metallurgy & Materials Processing, Shanghai University, Shanghai, China, 200072

Received: April 4, 2010; Revised Manuscript Received: April 20, 2010

The dehydrogenation properties and mechanism of $MgCl_2(NH_3)$/MBH_4 (here, M is Li or Na) were investigated by thermogravimetric analysis and mass spectrometry, X-ray diffraction (XRD), solid-state ^{11}B NMR, Fourier transform infrared, and differential scanning calorimetry (DSC). As for the $MgCl_2(NH_3)$/$LiBH_4$ system, it was found that a new phase, namely, $MgCl_2(NH_3)\cdot LiBH_4$, to which the following dehydrogenation relates, is formed after ball milling. Judging from the reaction products, it is confirmed that $MgCl_2$ is inclined to work as an ammonia carrier, and the ligand NH_3, transferring from $MgCl_2$, is able to combine with the $LiBH_4$ to release H_2 with a trace of ammonia at ca. 240 °C. With the increase of $LiBH_4$ content in the mixture, the emission of ammonia was totally suppressed, and $Mg(BH_4)_2$ was produced by the decomposition reaction of $MgCl_2$ with the excessive $LiBH_4$ after the ligand NH_3 was exhausted, resulting in an improved dehydrogenation in the whole system. As for the $MgCl_2(NH_3)$/$NaBH_4$ system, no new phases are detected by XRD after ball milling. The $MgCl_2$ works as a BH_4^- acceptor, and the ligand NH_3 stays with Mg^{2+} to combine with the BH_4^-, which transfers from $NaBH_4$ to Mg^{2+}, resulting in a totally different decomposition route and thermal effects as compared with the $MgCl_2(NH_3)$/$LiBH_4$ system. DSC results revealed that the decomposition of $MgCl_2(NH_3)$/$LiBH_4$ presented an exothermic reaction with an enthalpy of -3.8 kJ mol^{-1} H_2, while the $MgCl_2(NH_3)$/$NaBH_4$ showed two apparent endothermic peaks associated with its two-step dehydrogenation with enthalpies of 8.6 and 2.2 kJ mol^{-1} H_2, respectively. Moreover, the MS profiles of the $MgCl_2(NH_3)$/$2NaBH_4$, with excessive BH_4^-, still released a trace of NH_3, indicating that the $NaBH_4$ is not so effective in suppressing the emission of NH_3 as $LiBH_4$ did.

1. Introduction

Hydrogen is considered an ideal energy carrier candidate for future automotive applications that could be part of a carbon-free cycle. A key technical challenge in the way to a hydrogen-based energy economy is to develop a hydrogen storage system that provides a hydrogen source for on-board application with the features of safety and efficiency.[1−3] Among the various potential approaches, a number of physical, chemical, solid-state, and other approaches have been examined wildly without the successful implementation of such stores by any single material.[4] However, little attention has been paid to the possibility of using anhydrous ammonia, NH_3, which has a H_2 capacity as high as 17.6 wt % and is a lot easier to store in the solid state because of its polarity, as a medium for the storage of hydrogen onboard vehicles with the exception of the literature reported by Sorensen et al. Their work proposes that it is possible for metal ammine salts to work as safe, reversible, high-density, and low-cost hydrogen carriers, and in combination with an ammonia decomposition catalyst, the metal ammine salts, such as $MgCl_2(NH_3)_6$, which can store 9.1 wt % in the form of NH_3, provide a new solid hydrogen storage medium, working below 620 K.[5−9] However, given the catalytic decomposition of ammonia from the metal ammine salts, there are still many significant challenges, for example, high operation temperature and catalyst damage, that have to be overcome before it is available for an on-board application.

Recently, many promising hydrogen release materials, such as NH_3BH_3,[10,11] $Li(Na)NH_2BH_3$,[4,12] $Ca(NH_2BH_3)_2$,[13] and $Mg(BH_4)_2(NH_3)_2$[14] etc., have shown that negatively charged H in B−H and positively charged H in N−H may lead the dehydrogenation that takes place easily by the driving force of the redox reaction. It provides further approaches to release the hydrogen from the N−H group and brings new insights to develop a hydrogen-rich system based on the boron−nitrogen−hydrogen compounds. More recently, we have reported a new material system of $MgCl_2(NH_3)$/MBH_4 (M = Li, Na).[15] It has demonstrated that this novel system can work more efficiently as an ammonia-based indirect material for hydrogen storage based on a redox reaction.[16]

However, considered with a view to the practical application, further investigation on improving the hydrogen purity, suffering from the release of trace quantities of ammonia, is required. Moreover, as we have confirmed by XRD results in our previous publication, new phases were formed upon ball milling $MgCl_2(NH_3)_3$ with $LiBH_4$, showing interaction of these two chemicals, so further efforts should be carried out to characterize the starting materials and the reaction products, which is of considerable importance in an in-depth study for the mechanism on the dehydrogenation of the $MgCl_2(NH_3)$/$LiBH_4$.

In this paper, excessive $LiBH_4$ was used to suppress ammonia emission and to plot the pathway of ammonia emission from 1:1 $MgCl_2(NH_3)$/$LiBH_4$ in more detail. More than anything, we reveal the contrasting role that $LiBH_4$ and $NaBH_4$ play in

* To whom correspondence should be addressed. E-mail: yuxuebin@fudan.edu.cn.
[†] Fudan University.
[‡] Shanghai University.

10.1021/jp103012t
Published on Web 05/05/2010

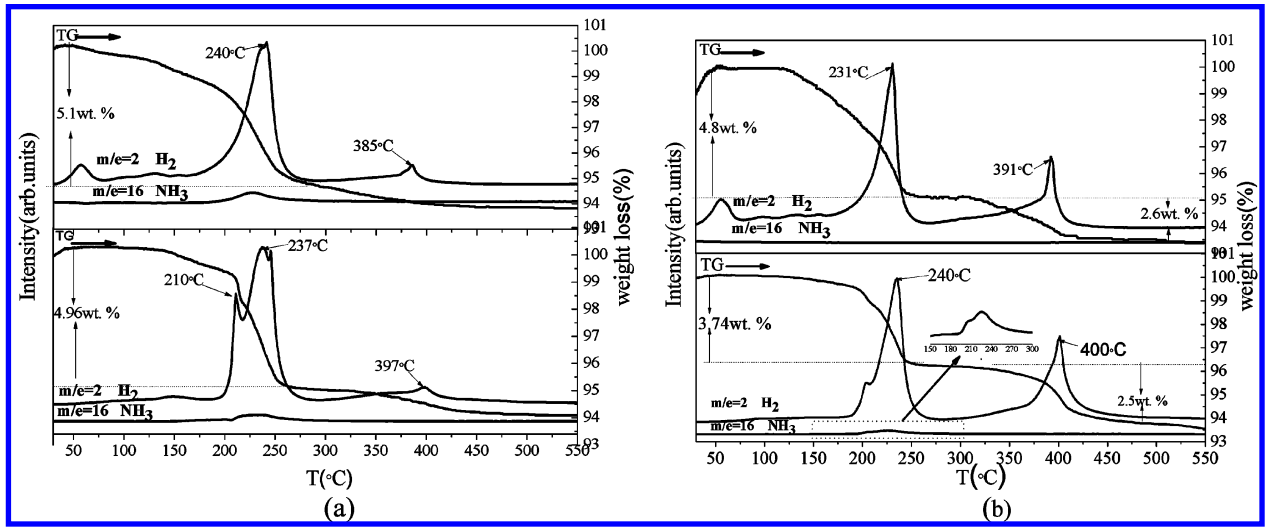

Figure 1. TGA-MS profiles for the hydrogen and ammonia release of the $MgCl_2(NH_3)/LiBH_4$ and $MgCl_2(NH_3)/NaBH_4$ with mole ratios of 1:1 (a) and 1:2 (b).

combining with the ligand ammonia. According to the post-milled phases, thermal performance, and reaction products, it was demonstrated that $MgCl_2(NH_3)$ and borohydrides combined into hydrogen in, at least, two alternative ways due to the difference in metal cations of the borohydrides; even the dehydrogenation occurred within a similar temperature range.

2. Experimental Methods

All samples were handled in an argon-filled glovebox, which kept both water and oxygen concentrations below 1 ppm during operation. Magnesium chloride (99%, Sigma Aldrich), sodium borohydride (97%, Sigma Aldrich), and lithium borohydride (97%, Sigma Aldrich) were used as received without further purification. Gaseous ammonia (99%) was dried by soap lime before use. $MgCl_2(NH_3)$ was prepared by heating $MgCl_2(NH_3)_6$ at 345 °C under 1 atm of ammonia atmosphere. The mixtures of $MgCl_2(NH_3)/LiBH_4$ and $MgCl_2(NH_3)/NaBH_4$ with various mole ratios were separately loaded into different milling vessels. The typical weight of samples was 1.5 g. The ball milling was conducted at 580 rpm for 6 min under an argon atmosphere by a SP2 planetary mill using an 80 mL stainless vial and balls. The vial was filled and sealed in a glovebox. The ratios of ball-to-powder were ca. 30:1.

Heat treatment of the samples was carried out in a closed test tube under argon atmosphere, and hydrogen was released into a carrier stream of argon through a T-joint with a thin connection tube to maintain the argon atmosphere over the samples. The typical time for heat treatment was 30 min.

Simultaneous thermogravimetric analysis and mass spectrometry (TGA-MS) were conducted under 1 atm of argon in the temperature range of room temperature and 600 °C at a heating rate of 10 °C min^{-1} using a netzsch STA 409 C analyzer equipped with a quadrupole mass spectrometer for the analysis of the evolved gas. Differential scanning calorimetry (DSC) was performed by high-pressure netzsch 204HP DSC under argon with a gas flow of 20 mL Ar min^{-1} at a heating rate of 10 °C min^{-1}. Hydrogen and ammonia release measurements were performed by TGA-MS using a heating rate of 10 °C min^{-1} under 1 atm of argon and a carrier flow rate of 200 cm^3 min^{-1}.

Powder X-ray diffraction (XRD) patterns were obtained with a Bruke X'PERT diffractometer (Cu Ka radiation, 16 Kw). During the XRD measurement, samples were mounted in a glovebox, and an amorphous polymer tape was used to cover the surface of the powder to avoid oxidation.

Solid-state infrared spectra of the samples (as KBr pellets) were recorded with a Nicolet Nexus 470 in the range of 1000−4000 cm^{-1}. During the IR measurements (KBr pellets), samples were loaded into one closed tube with CaF_2 windows.

The solid-state ^{11}B NMR was recorded (DSX 300) using a Doty CP-MAS probe with no probe background. All of the solid samples were spun at 12 kHz, using 4 mm ZrO_2 rotors filled up in purified argon atmosphere glove boxes. A 0.55 μs single-pulse excitation was employed, with repetition times of 1.5 s.

On the basis of the volumetric (TPD results) and gravimetric (TGA results) equations, the mole proportion of H_2 (C_{H_2}) and NH_3 (C_{NH_3}) released from the sample can be calculated from the following two equations:

$$C_{H_2} + C_{NH_3} = 1 \tag{1}$$

$$\left(C_{H_2} \times 2.02 + C_{NH_3} \times 17.03\right) \times M_p = W_p \tag{2}$$

where W_p is the weight loss from TGA results and M_p is the released gas volume (mol/g) from the TPD results.

3. Results and Discussion

3.1. H_2 and NH_3 Releases from $MgCl_2(NH_3)/LiBH_4$ and $MgCl_2(NH_3)/NaBH_4$ Systems. Figure 1a shows the TGA-MS profiles for the hydrogen and ammonia release of the $MgCl_2(NH_3)/LiBH_4$ (denoted as LB1) and $MgCl_2(NH_3)/NaBH_4$ (denoted as SB1), both with a mol ratio of 1:1. In the case of the LB1, the main H_2 desorption peak appears at 240 °C with an infinitesimally small NH_3 peak at 227 °C. The TGA-MS profile of SB1 shows two main H_2 peaks partly overlapping at 210 and 237 °C, consisting of at least a two-step dehydrogenation reaction, with a weak NH_3 peak at ca. 230 °C. The total weight loss before 300 °C is 4.96 wt %. On the basis of the TGA and volumetric results (not shown here), the quantitative decomposition capacities of H_2 and NH_3 released form LB1 and SB1 were calculated and are listed in Table 1. The calculation results indicate that the LB1 and SB1 release 2.91 and 2.57 equiv of H_2, accompanied by 0.08 and 0.1 equiv of NH_3 emission, correspond-

TABLE 1: Summary of the Decomposition Properties of $MgCl_2(NH_3)/LiBH_4$ and $MgCl_2(NH_3)/NaBH_4$

samples	peak temperature of dehydrogenation (°C)	TGA results (wt %)	ΔH (kJ/mol H_2)	H_2 (mol)/ sample (mol)	converted NH_3 (%)	XRD results
$Mg(NH_3)Cl_2/LiBH_4$ (mol ratio of 1:1)	240	5.1[a]	−3.8[a]	2.91 [a]	91.6[a]	$MgCl_2$ [a] LiCl [a,b]
$Mg(NH_3)Cl_2/LiBH_4$ (mol ratio of 1:2)	231, 391	4.8,[a] 2.6[b]		3.73,[a] 2 [b]	100	$LiMgCl_3$[a] Mg [b]
$Mg(NH_3)Cl_2/LiBH_4$ (mol ratio of 1:3)	229, 397, 434[c]	3.1,[a] 3.7,[b] 1[c]		2.25,[a] 2.68,[b] 0.73 [c]	100	LiCl [a] Mg [b]
$Mg(NH_3)Cl_2/NaBH_4$ (mol ratio of 1:1)	(210, 237)[a]	4.96,[a] 0.93[b]	10.8[a]	2.57[a]	84.3[a]	NaCl[a]
$Mg(NH_3)Cl_2/NaBH_4$ (mol ratio of 1:2)	(201, 240),[a] 400	3.74,[a] 2.5[b]	10.4[a]	2.54[a] 2.97[b]	88.6[a]	NaCl [a], [b], Mg[b], $NaBH_4$ [a]

[a] The results were detected corresponding to the first dehydrogenation step. [b] The results were detected corresponding to the second dehydrogenation step. [c] The results were detected corresponding to the decomposition of $LiBH_4$.

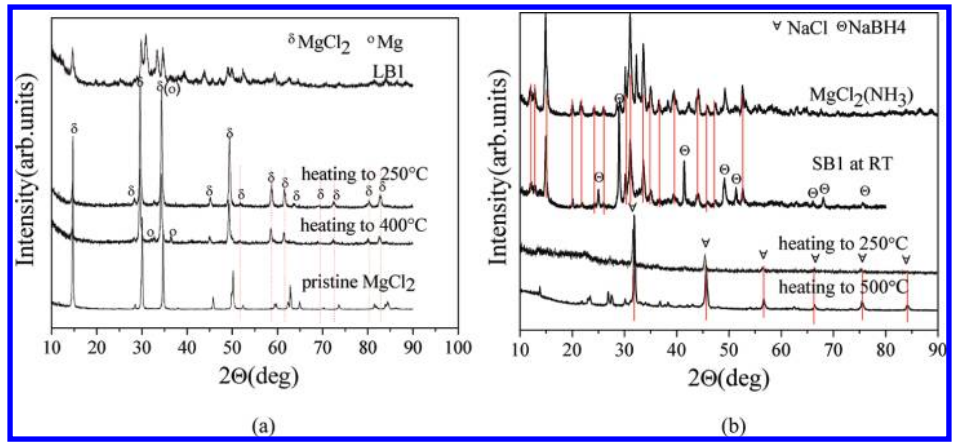

Figure 2. XRD patterns of the as-prepared $MgCl_2(NH_3)/LiBH_4$ (mol ratio of 1:1) (a) and $MgCl_2(NH_3)/NaBH_4$ (mol ratio of 1:1) (b) after heating to various temperatures.

ing to 91.6 and 84.3% NH_3 conversion for LB1 and SB1, respectively.

To further confirm the role of the BH_4^- anion in ammonia suppression, the performance of H_2 and NH_3 release from $MgCl_2(NH_3)/2LiBH_4$ (with a mol ratio of 1:2, denoted as LB2) and $MgCl_2(NH_3)/2NaBH_4$ (with a mol ratio of 1:2, denoted as SB2) was also characterized by TGA-MS. Figure 1b again compares the H_2 and NH_3 release of LB2 and SB2 side by side. It is obvious that the dehydrogenation process from both systems is similar. As compared to the MS result of LB1, NH_3 is totally suppressed, with two major H_2 peaks observed at 231 and 391 °C, respectively. The TGA curve of LB2 shows that the hydrogen release capacities for the two steps are about 4.8 and 2.6 wt %, respectively, corresponding to 3 and 2 equiv of H_2. The enhancement of H_2 purity should be due to the excessive $LiBH_4$. However, in the case of SB2, a trace amount of NH_3 was still detected along with two main H_2 peaks observed at 240 and 400 °C (Figure 1b), resulting in impurity of H_2. By the volumetric and gravimetric results, the efficiency of ammonia conversion of SB2 was calculated to be 88.6%, a little higher than SB1 but never advancing as high as LB2.

3.2. Phase Transformation and Thermal Performance of $MgCl_2(NH_3)/LiBH_4$ and $MgCl_2(NH_3)/NaBH_4$ Systems. The XRD patterns and ^{11}B NMR results provided the information of phase transformation and chemical environment of B atoms for both LB1 and SB1 after ball milling and heating to 250 and 500 °C. As shown in Figure 2a, after ball milling, new peaks, which correspond to neither $LiBH_4$ nor $MgCl_2(NH_3)$ and cannot be identified in the database, were detected for LB1. However, given the low purity and poor crystallizability of this novel $MgCl_2(NH_3)\cdot LiBH_4$ phase prepared by ball milling, it is difficult to determine the accurate structure of the new compound, and further investigation, for example, high-revolution XRD and structure solution, is required to understand the nature of the reaction. Even so, the ^{11}B NMR and Fourier transform infrared (FTIR) results show no observed chemical shifting of B atoms as compared to the BH_4^- and barely detectable changes in the peak position of N−H bonding as compared to the $MgCl_2(NH_3)$ (see the later discussion). These results safely confirm some key information for the postmilled $MgCl_2(NH_3)/LiBH_4$: (1) Both the BH_4^- and the ligand NH_3 subunits remain intact in their own structure; (2) as compared to the substance, there should be no change in the chemical composition.

So, we surmise that ball milling may result in the formation of a new phase with the ligand NH_3 and BH_4^- mixed on a molecular scale but without further combination issuing in the formation of any BN chemicals. The information gathered above suggests that the complex of $MgCl_2(NH_3)\cdot LiBH_4$, to which the follow-up dehydrogenation at low temperature should be related, was formed during ball milling. Combined with our previous report, the pathway of H_2 release form LB1 can be modified as:

$$MgCl_2(NH_3) + LiBH_4 \xrightarrow{\text{ball milling}} MgCl_2(NH_3)\cdot LiBH_4 \rightarrow MgCl_2 + LiBNH + 3H_2 \quad (3)$$

However, it is noteworthy that, in the XRD profile of the as-prepared SB1, the phase of $NaBH_4$ can be identified easily and the $MgCl_2(NH_3)$ phase was retained clearly but with a lower intensity as compared to the pristine one. Surprisingly, the XRD patterns confirmed that no new phase was formed by ball milling, suggesting that the dehydrogenation of $MgCl_2(NH_3)/NaBH_4$ is most likely to be ascribed to the direct combination

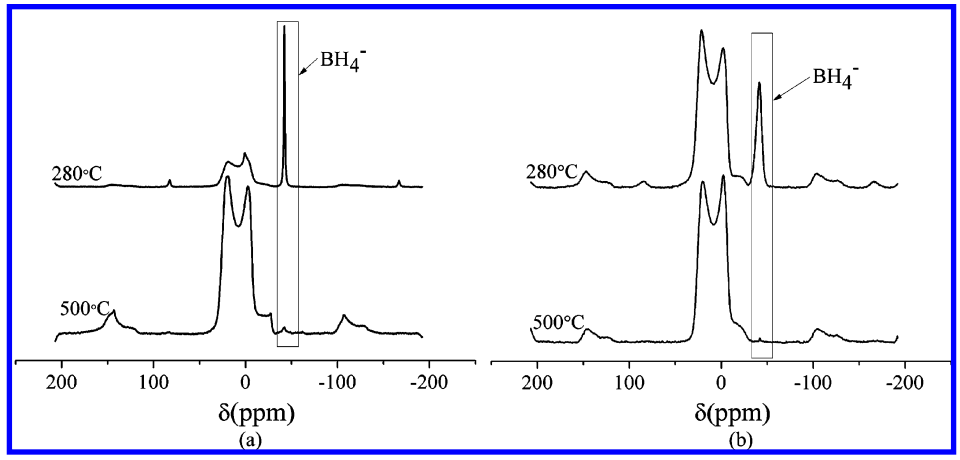

Figure 3. ^{11}B NMR of (a) $MgCl_2(NH_3)/LiBH_4$ (mol ratio of 1:1) and (b) $MgCl_2(NH_3)/NaBH_4$ (mol ratio of 1:1) after heating to 280 and 500 °C.

of the dissociative $MgCl_2(NH_3)$ and $NaBH_4$ without keeping the ligand NH_3 and BH_4^- in a molecular level. These results imply that as compared to the $NaBH_4$, $LiBH_4$ is able to bond with NH_3 via the lone electronic pairs.[17] More details of the chemical pathway and the amorphous end product can be deduced by the solid-state ^{11}B NMR results of the LB1 and SB1 after heating at 280 and 500 °C, as shown in Figure 3. For the two samples, after heating to 280 °C, the presence of a sharp line at ca. 42.0 ppm, assigned to the B nucleus in the tetrahedral BH_4^- unit, implies that partial BH_4^- fails to react with the ligand NH_3, resulting in the NH_3 signal observed in the MS.[15] In the case of the LB1, two peaks of tridentate B nucleus can be observed at 17.2 and 2.4 ppm; these peaks are most likely to be part of a single quadrupolar resonance or possibly two overlapping quadrupolar resonances. Gervais et al. have presented similar resonances at a variety of field strengths, confirming the formation of BN_3 or BN_2H or even a mixture of both.[18] As for SB1 after heating to 280 °C, two extremely similar peaks were observed for the chemical shift of B (observed at 19.1 and 0.8 ppm; see Figure 3), implying that no matter which borohydride was employed, the dehydrogenation of both LB1 and SB1 should be ascribed to the combination of BH_4^- with the ligand NH_3. However, these two signals of BN_3 and BN_2H are difficult to identify from the 7.01 T NMR spectrum because of the large quadrupolar interaction that broadens the peaks over a much larger chemical shift range. Because the different sensitivity of tricoordination (BN_3 or BN_2H) and tetracoordinated (BH_4) to the perturbation and the higher field NMR should be effective to weaken the quadrupolar interaction of B (spin = 3/2), further identification for the BN_3 and BN_2H by performing ^{11}B NMR at varied fields is required.

The FTIR spectrum of SB1 in Figure 4 suggests that the ligand NH_3 and BH_4^- anions remain intact within the molecular structure after mixing together at room temperature as demonstrated by the XRD results.[19] After heating to 250 °C, the positions of these bands are not markedly different from those measured for the 1:1 $MgCl_2(NH_3)/NaBH_4$ mixture, while the dramatic decay of intensity of the bands in the NH_2 and BH_2 bending and BH stretching region is observed, suggesting the chemical combination of the ligand NH_3 and BH_4 anions, which agrees with the dehydrogenation process of SB1.

The DSC results in Figure 5 and reaction products observed in XRD patterns in Figure 2 further confirm the discrepancy in the dehydrogenation pathway between the $MgCl_2(NH_3)/LiBH_4$ and the $MgCl_2(NH_3)/NaBH_4$ systems. As for the LB1, the DSC shows one broadened endothermic peak in the range of ca. 60

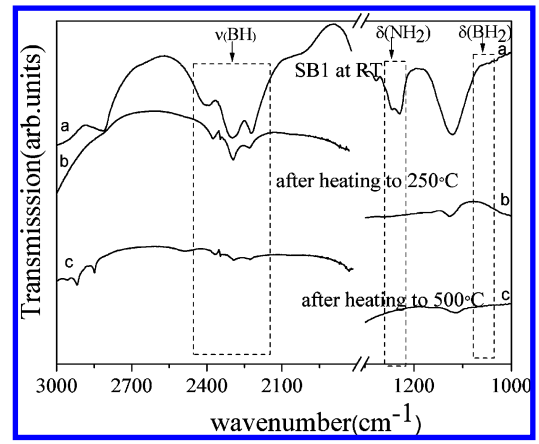

Figure 4. IR spectra for $MgCl_2(NH_3)/NaBH_4$ (mol ratio of 1:1) (a) at room temperature, (b) after heat treatment at 250 °C, and (c) after heat treatment at 500 °C.

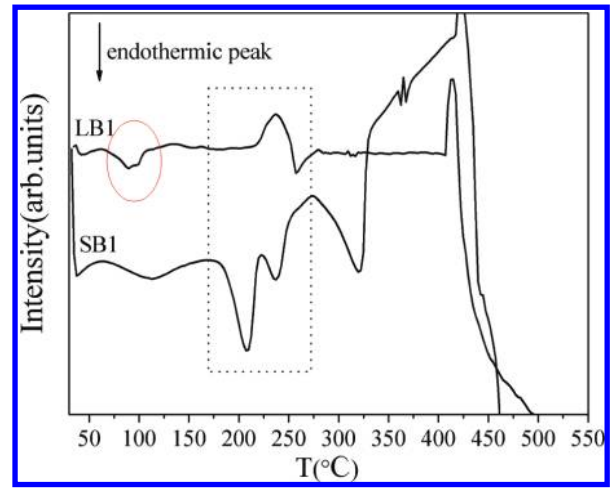

Figure 5. DSC results of $MgCl_2(NH_3)/LiBH_4$ (denoted as LB1) and $MgCl_2(NH_3)/NaBH_4$ (denoted as SB1). Both samples had a mol ratio of 1:1.

and 108 °C with a maximum at ca. 89 °C, which should be assigned to the phase transformation of $MgCl_2(NH_3)\cdot LiBH_4$ instead of $LiBH_4$ or $MgCl_2(NH_3)$, while no such peaks were observed in the DSC profile of SB1. In the main range of dehydrogenation, the main exothermic peak of LB1 lies at 240 °C, which is consistent with the MS results. Using the peak fitting method along with the H_2 amount released until 260 °C, the enthalpy of this step dehydrogenation was estimated to be

−3.8 kJ mol^{-1} H_2, significantly less exothermic than from the pristine NH_3BH_3 (−20 kJ mol^{-1} H_2)[10,11] but very close to that of Li(Na)NH_2BH_3 (−3 to −5 kJ mol$^{-1}H_2$),[4] suggesting, in common with the substitution of H by Li^+ or Na^+, that the formation of the $MgCl_2(NH_3)\cdot LiBH_4$ phase will induce considerable modification of the chemical bonding between H^- in BH_4 and H^+ in NH_3. It can be deduced that enthalpy desorption, produced by the combination of H^- in BH_4^- and H^+ in NH_3, may be the driving force of eq 3. While, interestingly, the DSC curve of $MgCl_2(NH_3)/NaBH_4$ (1:1), which consists of the same BH_4^- and NH_3 units as ones in the $MgCl_2(NH_3)/LiBH_4$ (1:1), shows two endothermic peaks with a desorption enthalpy of 10.8 kJ mol^{-1} H_2. Combined with the fact that only crystal $MgCl_2$ and NaCl are detected by XRD for the dehydrogenated LB1 and SB1, it is suggested that the ligand NH_3 and BH_4^- combining may occur around Li^+ and Mg^{2+} in the LB1 and SB1, respectively. This surmise is also supported by the similar thermal difference observed between the Li−B−N−H system, that is, $LiNH_2BH_3$ (exothermic) and $Li_3BN_2H_8$ (exothermic),[16,20] and the Mg−B−N−H system, that is, $Mg(BH_4)_2\cdot 2NH_3$ (endothermic).[14]

Equation 3 has confirmed that $MgCl_2$ is inclined to work as an ammonia carrier, and the ligand NH_3, transferring from $MgCl_2$, is able to combine with the $LiBH_4$ to release H_2. While coming to $MgCl_2(NH_3)/NaBH_4$, all of the experimental results above imply that the $MgCl_2$ works as a BH_4^- acceptor, and the ligand NH_3 stays with Mg^{2+} to combine with the BH_4^-, which transfers from $NaBH_4$ to Mg^{2+}, resulting in a totally different decomposition route and thermal effects as compared with the $MgCl_2(NH_3)/LiBH_4$ system. The main reaction products after dehydrogenation are NaCl and H_2 with one amorphous phase with the elementary constituent of MgBNH or MgBNHCl. Even without enough composition and valent information for this amorphous phase, considering the conservation of elements and the balancing of the chemical reaction, it may be more reasonable to identity the end product as MgBNHCl. The product after dehydrogenation deduced by XRD and DSC results and releasing about 3 equiv of H_2 suggests that eq 4 has occurred.

$$MgCl_2(NH_3) + NaBH_4 \rightarrow MgCl(BNH) + NaCl + 3H_2 \quad (4)$$

The calculated weight loss of eq 4 ascribed to H_2 release is ca. 4 wt %, which is 0.96 wt % lower than the result of TGA due to the release of a trace of NH_3 (note that NH_3 is much heavier than H_2).

Even eqs 3 and 4 play dominant roles for the H_2 evolution from the $MgCl_2(NH_3)/LiBH_4$ and $MgCl_2(NH_3)/NaBH_4$; the following extra discrepancy should be elaborated further: (1) the pathway of the ammonia emission for this two systems; (2) the B site of BH_4 observed in the ^{11}B NMR spectra of postheated LB1 and SB1 at 250 °C; (3) the possible reason for the 0.4−1.0° down-shifting for XRD peaks of the crystal product for $MgCl_2(NH_3)/LiBH_4$, which we surmise as $MgCl_2$; and (4) the observed H_2 signal at ca. 385 and 397 °C for $MgCl_2(NH_3)/LiBH_4$ and $MgCl_2(NH_3)/NaBH_4$, respectively.

The MS signals of pure $Mg(NH_3)Cl_2$ show a weak peak corresponding to NH_3 release at around 227 °C, consistent with the main emission of NH_3 in LB1 detected at around 227 °C.[15] The thermodynamic similarity in NH_3 release reveals that the mechanism of ammonia emission in LB1 is nearly the same as the decomposition of pure $Mg(NH_3)Cl_2$. Many hypothetical mechanisms may be responsible for the formation of BH_4^- anion and the emission of ammonia. However, there are at least two qualifications with which the mechanisms should be consistent: (1) Apart from the BH_4^-, nearly all of the B atoms in the decomposition product of LB1 are only in trigonal planar HBN_2 or BN_3 environments, and (2) it is highly possible that the emission of NH_3 comes from the ligand NH_3 in $Mg(NH_3)Cl_2$. Maybe, as we have surmised in our previous literature, the emission of NH_3 of LB1 is due to incomplete contact of the particles in the solid state, and the ligand NH_3 fails to take chemical eq 3 with $LiBH_4$.[15] A similar reason can be adequate for the SB1. According to the previous literature,[21,22] the remaining $LiBH_4$ will take chemical eq 5 with $MgCl_2$, which is the decomposition of $Mg(NH_3)Cl_2$, as follows:

$$2MgCl_2 + 2LiBH_4 \rightarrow Mg(BH_4)_2 + MgLiCl_3 + LiCl \quad (5)$$

So, we suggest that the final solid product of LB1 after thermal decomposition is the coexistence of $LiMgCl_3$, $MgCl_2$, and LiCl, which may be responsible for the XRD peaks shifted to a low-angle by the mechanism of $LiMgCl_3$, $MgCl_2$, and LiCl solid solutions, resulting in the formation of $Mg_xLi_{2(1-x)}Cl_2$. The existence of $Mg(BH_4)_2$ should be responsible for the B site of BH_4^- observed in the ^{11}B NMR spectra of the postheated LB1 at 250 °C. After further heating to 500 °C, the BH_4^- peak disappeared totally, suggesting the decomposition of $Mg(BH_4)_2$, so the observed small peak in the MS signal of H_2 at around 390 °C (see Figure 1) can be explained by eq 6:

$$Mg(BH_4)_2 \rightarrow Mg + 2B + 4H_2 \quad (6)$$

which explains the presence of the Mg phase after heat treatment at 390 °C, again consistent with the presence of $Mg(BH_4)_2$ in eq 5 (see Figure 2a). Oddly, MgH_2, which has been widely taken as an intermediate product during the decomposition of $Mg(BH_4)_2$, is never observed. It is noteworthy that the absence of the BH_4^- peak in ^{11}B is also observed by further heating SB1 to 500 °C, implying that the small H_2 peak can be safely ascribed to the decomposition of BH_4^- unit (see Figure 3).

To further verify eqs 3−6, the phase transformation of LB2 and SB2 was also investigated by XRD. In the case of the LB2, besides the phase of excessive $LiBH_4$, the XRD patterns of the postmilled LB2 show that the $MgCl_2(NH_3)\cdot LiBH_4$ phase was formed with higher purity and intensity, and no $MgCl_2(NH_3)$ was observed (see Figure 6). As for the SB2, $MgCl_2(NH_3)$ and $NaBH_4$ still can be identified. This kind of striking difference in the formation of $MgCl_2(NH_3)\cdot LiBH_4$ and the failure to produce the $MgCl_2(NH_3)\cdot NaBH_4$ may be attributed to the different efficiency of ammonia suppression between $LiBH_4$ and $NaBH_4$. After heat treatment of LB2 at 240 °C, a solid-state mixture is obtained, which clearly consists of $MgLiCl_3$ and LiCl phases characterized by XRD (see Figure 5), again consistent with eq 5. The reason for the absence of $Mg(BH_4)_2$ may be due to the fact that the compound synthesized by this method did not crystallize sufficiently; the same results have been confirmed by Matsunaga et al.[22] The TGA result at 240 °C, giving about 1.5 equiv of H_2 for LB2 during the first dehydrogenation step, is consistent with the eq 3. Coming to the SB2, after heating to 250 °C, NaCl and $NaBH_4$ phases were observed, in agreement with eq 4. Further heating to 500 °C, Mg was present.

To further confirm the $MgCl_2$, which plays a crucial role in plotting the dehydrogenation path of $MgCl_2(NH_3)/LiBH_4$, phase analysis of 1:3 $MgCl_2(NH_3)/LiBH_4$ (denoted as LB3) was carried

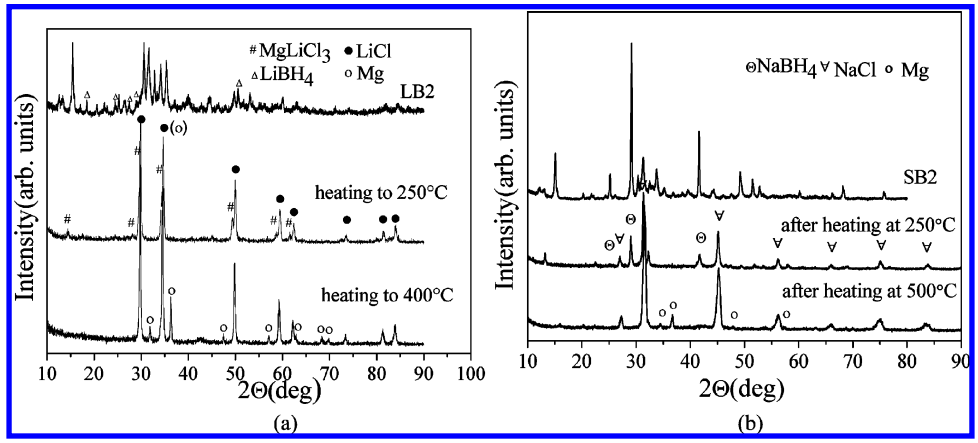

Figure 6. XRD results for (a) $MgCl_2(NH_3)/LiBH_4$ (mol ratio of 1:2) at room temperature and after heating to 250 and 400 °C and (b) $MgCl_2(NH_3)/NaBH_4$ (mol ratio of 1:2) at room temperature and after heating to 250 and 500 °C.

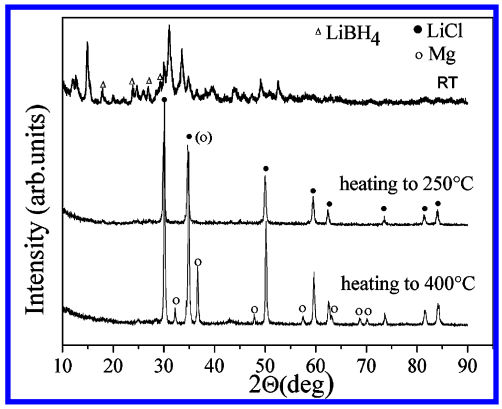

Figure 7. XRD results for $MgCl_2(NH_3)/LiBH_4$ (mol ratio of 1:3) at room temperature and after heating to 250 and 400 °C.

out. The reason for this choice is that, as well recognized, 1:2 is the stoichiometric proportion for the interaction between $MgCl_2$ and $LiBH_4$, so it can be expected that any $MgCl_2$, which has been supposed as the reaction product of LB1, would transform to LiCl due to the eq 7:

$$MgCl_2 + 2LiBH_4 \rightarrow LiCl + Mg(BH_4)_2 \qquad (7)$$

The XRD results for LB3 (Figure 7) show that only the LiCl phase remained as expected after heating to 250 °C. After further heating to 400 °C, Mg was detected, again in agreement with eq 6. It has been supposed that the possibility of $MgCl_2-LiCl$ solid solutions, similar to that that occurs to $LiCl-LiBH_4$,[23] may be responsible for the peak shifts of $MgCl_2$. Granted, further experiments, namely, the phase analysis of reaction products of LB3, have safely confirmed the identification of $MgCl_2$.

3.3. Discussion. It is clear that the different dehydrogenation routes between the $MgCl_2(NH_3)/NaBH_4$ and the $MgCl_2(NH_3)/LiBH_4$ systems should be considered as two typical chemical reactions between NH_3 and borohydrides. Even though it is difficult to explain the detailed reaction mechanism and the dehydrogenation products without enough electronic and structural change information, it is concluded that the different activities of electron-accepting ions (Na^+ and Li^+) should be the main reasons for the total different chemical pathway. Among the three metal cations (Mg^{2+}, Li^+, and Na^+), Mg^{2+} is the strongest Lewis acid. Therefore, the NH_3, which is normally a ligand due to its lone electronic pairs, should be more inclined to coordinate with Mg^{2+}. In other words, in the system of $MgCl_2(NH_3)/MBH_4$ (here M is Li or Na), the ligand NH_3 does not likely transfer from $MgCl_2$ to the Li or Na cation, generating a H_3NLi^+ or H_3NNa^+ group. However, it should not be neglected that B−H bonds in BH_4^- are also very competitive with these metal cations to combine with NH_3 by the agency of N−H···H−B dihydrogen bonds. As one wildly existent bonding force between BH_4^- and NH_3, for example, $LiBH_4NH_3$,[17] $Ca(NH_2BH_3)_2(NH_3)_2$,[24] $Mg(BH_4)_2(NH_3)_2$,[14] and $Al(BH_4)_3(NH_3)_6$,[25] etc., it definitely plays a crucial role in determining the decomposition routes of $MgCl_2(NH_3)/MBH_4$. So, M^+ and BH_4^- work together to attack the ligand NH_3, and conversely, NH_3 can also join up to combine with BH_4^-. As compared with Na^+, Li^+ is a stronger Lewis acid due to smaller ion radii and, with the concerted efforts of BH_4^-, is able to acquire the lone electron pair of the ligand NH_3. Therefore, as we have surmised in eq 3, subsequently, NH_3 transfers from $MgCl_2$ to combine with $LiBH_4$. The N−H···H−B dihydrogen bonds weaken the Li−N bonds sharply. Coming to the $MgCl_2(NH_3)/NaBH_4$ system, as an electron acceptor, Na^+ seems too weak to dispute the NH_3 with Mg^+, even with the "help" of BH_4^-. Instead, the BH_4^- is most likely to gravitate to Mg^+ to form $Mg(BH_4)Cl\cdot xNH_3$.

4. Conclusion

In the present study, the dehydriding pathways of $MgCl_2(NH_3)/MBH_4$ (M is Li or Na) with various mole ratios were studied systemically. The mechanical ball milling of $MgCl_2(NH_3)/LiBH_4$ results in the formation of a new phase, namely, $MgCl_2(NH_3)\cdot LiBH_4$, to which the following dehydrogenation relates. Along with the increase of the $LiBH_4$ content in the mixture, the emission of ammonia is totally suppressed, and $Mg(BH_4)_2$ was produced by the decomposition reaction of $MgCl_2$ with excessive $LiBH_4$ after the ligand NH_3 was exhausted, resulting in an improved dehydrogenation in the whole system. DSC results revealed that this reaction is an exothermic reaction, and the enthalpy for the dehydrogenation in $MgCl_2(NH_3)/LiBH_4$ (mol ratio of 1:1) is −3.8 kJ mol^{-1} H_2. While, in the case of the $MgCl_2(NH_3)/NaBH_4$, no phase transition was observed. The main decomposition pathway of the 1:1 $MgCl_2(NH_3)/NaBH_4$ mixture ultimately yields amorphous MgBNHCl or MgBNH along with NaCl via intermediate formation of the ammine magnesium borohydrides complex $Mg(BH_4)Cl\cdot xNH_3$, which showed an endothermic reaction with an enthalpy of 10.8 kJ mol^{-1} H_2. Further investigation revealed that the $MgCl_2(NH_3)/NaBH_4$ system has not shown the same efficiency as the $MgCl_2(NH_3)/LiBH_4$ system in depressing the emission of

ammonia. In the case of the $MgCl_2(NH_3)/NaBH_4$ (1:2), the emission of ammonia is still observed. It is believed that this kind of striking difference in the efficiency of ammonia suppression between $LiBH_4$ and $NaBH_4$ may be due to the formation of $MgCl_2(NH_3)\cdot LiBH_4$ and the failure to produce the $MgCl_2(NH_3)\cdot NaBH_4$. Basically, the substantially different decomposition pathways in $MgCl_2(NH_3)/LiBH_4$ and $MgCl_2(NH_3)/NaBH_4$ are due to the different activities of electron-accepting ions (Na^+ and Li^+), to which the BH−NH group is close on a molecular level, and may dominate the thermal performance of the dehydrogenation.

Acknowledgment. This work was partially supported by the Program for New Century Excellent Talents in University (NCET-08-0135), the Ph.D. Programs Foundation of Ministry of Education of China (20090071110053), and the Shanghai Leading Academic Discipline Project (B113) and Pujiang Programs (08PJ14014).

References and Notes

(1) Schlapbach, L.; Züttel, A. *Nature* **2001**, *414*, 353–358.

(2) Grochala, W.; Edwards, P. P. *Chem. Rev.* **2004**, *104*, 1283–1315.

(3) Bogdanovic, B.; Felderhoff, M.; Kaskel, S.; Pommerin, A.; Schlichte, K.; Schuth, F. *Adv. Mater.* **2003**, *15*, 1012–1015.

(4) Xiong, Z. T.; Yong, C. K.; Wu, G. T.; Chen, P.; Shaw, W.; Karkamkar, Autrey, A. T.; Jones, M. O.; Johnson, S. R.; Edwards, P. P.; David, W. I. F. *Nat. Mater.* **2008**, *7*, 138–141.

(5) Sørensen, R. Z.; Hummelshøj, J. S.; Klerke, A.; Reves, J. B.; Vegge, T.; Nørskov, J. K.; Christensen, C. H. *J. Am. Chem. Soc.* **2008**, *130*, 8660–8668.

(6) Christensen, C. H.; Sørensen, R. Z.; Johannessen, T.; Quaade, U. J.; Honkala, K.; Elmøe, T. D.; Køhlera, R.; Nørskov, J. K. *J. Mater. Chem.* **2005**, *15*, 4106–4108.

(7) Hummelshøj, J. S.; Sørensen, R. Z.; Kustova, M. Y.; Johannessen, T.; Nørskov, J. K.; Christensen, C. H. *J. Am. Chem. Soc.* **2006**, *128*, 16–17.

(8) Christense, C. H.; Johannessen, T.; Sørensen, R. Z.; Nørskov, J. K. *Catal. Today* **2006**, *111*, 140–144.

(9) Klerke, A.; Christensen, C. H.; Nørskov, J. K.; Vegge, T. *J. Mater.Chem.* **2008**, *18*, 2304–2310.

(10) Stephens, F. H.; Pons, V.; Baker, R. T. *Dalton Trans.* **2007**, *25*, 2613–2626.

(11) Wolf, G.; Baumann, J.; Baitalow, F.; Hoffman, F. P. *Thermochim. Acta* **2000**, *343*, 19–25.

(12) Kang, X.; Fang, Z.; Kong, L.; Cheng, H.; Yao, X.; Lu, G.; Wang, P. *Adv. Mater.* **2008**, *20*, 2756–2759.

(13) Diyabalanage, H. V. K.; Shrestha, R. P.; Semelsberger, T. A.; Scott, B. L.; Bowden, M. E.; Davis, B. L.; Burrell, A. K. *Angew. Chem., Int. Ed.* **2007**, *46*, 8995–8997.

(14) Soloveichik, G.; Her, J. H.; Stephens, P. W.; Gao, Y.; Rijssenbeek, J.; Andrus, M.; Zhao, J. C. *Inorg. Chem.* **2008**, *47*, 4290–4298.

(15) Gao, L.; Guo, Y. H.; Xia, G. L.; Yu, X. B. *J. Mater. Chem.* **2009**, *19*, 7826–7829.

(16) Chater, P. A.; Dvaid, W. I. F.; Johnson, S. R.; Edwards, P. P.; Anderson, P. A. *Chem. Commun.* **2006**, *23*, 2439–2441.

(17) Johnson, S. R.; David, W. I. F.; Royse, D. M.; Sommariva, M.; Tang, C. Y.; Fabbiani, F. P. A.; Jones, M. O.; Edwards, P. P. *Chem. Asian J.* **2009**, *4*, 849–854.

(18) Gervais, C.; Maquet, J.; Babonneau, F.; Duriez, C.; Framery, E.; Vaultier, M.; Florian, P.; Massiot, D. *Chem. Mater.* **2001**, *13*, 1700–1707.

(19) Marks, T. J.; Klob, J. R. *Chem. Rev.* **1977**, *77*, 263–293.

(20) Nakamori, Y.; Ninomiya, A.; Kitahara, G.; Aoki, M.; Noritake, T.; Miwa, K.; Kojima, Y.; Orimo, S. *J. Power Sources* **2006**, *155*, 447–455.

(21) Chłopek, K.; Frommen, C.; Leon, A.; Zabara, O.; Fichtner, M. *J. Mater. Chem.* **2007**, *17*, 3496–3503.

(22) Matsunaga, T.; Buchter, F.; Miwa, K.; Towata, S.; Orimo, S.; Zuttel, A. *Renewable Energy* **2008**, *33*, 193–196.

(23) Arnbjerg, L. M.; Ravnsbæk, D. B.; Filinchuk, Y.; Vang, R. T.; Cerenius, Y.; Besenbacher, F.; Jørgensen, J.; Jakobsen, H. J.; Jensen, T. R. *Chem. Mater.* **2009**, *21*, 5772–5782.

(24) Chua, Y. S.; Wu, G. T.; Xiong, Z. T.; He, T.; Chen, P. *Chem. Mater.* **2009**, *21*, 4899–4904.

(25) Lovkovskii, E.; Polyakova, V.; Shilkin, S.; Semenenko, K. *J. Struct. Chem.* **1975**, *16* (1), 66–72.

JP103012T